PAPER • OPEN ACCESS

Study on the effect of lithium nitrate in ionic conduction properties based alginate biopolymer electrolytes

View the article online for updates and enhancements.
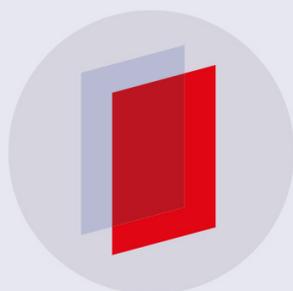
Materials Research Express

PAPER

Study on the effect of lithium nitrate in ionic conduction properties based alginate biopolymer electrolytes

A F Fuzlin[1], N A Bakri[1], B Sahraoui[2] and A S Samsudin[1]

[1] Ionic Materials Team, Faculty of Industrial Sciences and Technology, Universiti Malaysia Pahang, 26300 Pahang, Malaysia
[2] Université d'Angers, CNRS UMR 6200, Laboratoire MOLTECH-Anjou, 2 bd Lavoisier, 49045 ANGERS cedex, France

E-mail: ahmadsalihin@ump.edu.my

Abstract

In this present work, the conduction properties of biopolymer electrolytes (BEs) based alginate incorporation with $LiNO_3$ was studied. FTIR analysis showed there is complexation occurred when incorporation with $LiNO_3$ via COO^- group of alginate. The interaction between alginate and $LiNO_3$ shown an improvement in ionic conductivity of BEs where was increased from $3.24 \times 10^{-7} \, S \, cm^{-1}$ for un-doped sample and achieved optimum value at $1.14 \times 10^{-4} \, S \, cm^{-1}$ for sample containing with 15 wt. % $LiNO_3$. The prepared samples shown that it has thermally assisted when the temperature is increased and shown Arrhenius behavior. Deconvolution approached revealed that the present ionic conduction of BEs influenced by ionic mobility and diffusion coefficient.

1. Introduction

In recent days, synthetic polymer become main worldwide focus in electrolyte study due to good performance, high energy density, flexibility, and long life span in electrochemical device [1]. However, synthetic polymer itself contributed environmental pollution to the Earth. For example, petroleum derived plastic are not biodegradable, they do not go through microbial degradation and just dispersed to the ecosystem. The disadvantages of using the synthetic polymer in electrochemical device are non-environmental friendly, high cost production, less permeability and harmful to use [2]. Even though it provides excellent rechargeable-high density of energy that is portable, an issue using non-degradable in the device has definitely cause damage to the environment due to toxic monomer release [3]. It became an important issue to develop good protonic conducting polymer electrolyte with good aspect performance. Therefore, in order to rectify this problem, the renewable resources have been drawn in electrochemical industry, which can degrade to environment easily without generating harmful and toxic residues [4].

Biopolymer become main focusing area in industry to build green world in order to avoid all the profanation environment and energy disaster. For example, the biodegradable polymer already been used in industry of packaging, pharmaceutical, agriculture, tissue engineering, thickening agent, and biomedical. Biopolymer is suitable to been focused widely in electrochemical industry due to great ability to degrade in the long term which reduces the environmental effect [5]. Biopolymer materials are found to be easy undergoing degradation and compostable under normal environment condition; which showed that biopolymers more environmental friendly compared to synthetic polymers.

In the present work, alginate was chosen as host polymer due to anionic structure of polysaccharides composed of linear $(1 - >4)$ β-D-mannuronic acid (M) and α-L-guluronic acid (G) residues where capable of ionically crosslinking in the presence of cations [6]. Moreover, alginate polymer exhibits standard film properties like non-toxicity, good solubility, high mechanical strength, and biocompatible [7]. Due to advantages such as no-leakage of electrolyte, flexible geometry, higher energy density, and improved safety hazards in Li^+ ions batteries [8, 9]. The typical technique for obtaining favorable conduction properties of polymer electrolytes (PEs) is by incorporating with alkali metal salts (including lithium salts). The development of lithium-ion based PEs has shown great attention due to their stability in energy storage application [10]. The

Table 1. List of samples with their compositions respectively.

Designation	Weight percentage (wt%)
ALNO-0	0
ALNO-1	5
ALNO-2	10
ALNO-3	15
ALNO-4	20
ALNO-5	25

weak coordination in presence of salt $LiNO_3$ makes possible incorporation of Li^+ ion with the polar group of alginate polymer, which promotes charge carrier to polymer matrix and increase the ionic conduction [11]. This type of lithium salt ($LiNO_3$) might provide good complexation with polymer backbone due to its electronegativity and delocalization of charge [12]. The aim of this research is to study the conduction properties of based on effect of $LiNO_3$ in alginate as biopolymer electrolytes (BEs) system. The prepared sample of BEs system with different composition of $LiNO_3$ were investigated by using Fourier Transform Infrared (FTIR) spectroscopy and Electrical Impedance Spectroscopy (EIS). In addition, the determination of ionic transport properties of present BEs via FTIR vibrational effect which was evaluated based deconvolution approach provides considerable new insights into the conduction of ions that dissociate in the BEs system.

2. Experimental

2.1. Preparation of biopolymer electrolytes

In this work, alginate (Shaanxi Orient Co.) and $LiNO_3$ (Sigma Aldrich Co.) were used for preparation as biopolymer electrolytes (BEs) film. By employing solution-casting technique, 2 g of alginate was dissolved in distilled water. Then, different composition of $LiNO_3$ were added into the alginate solution and stirred until became homogenous solution. A homogenous solution was casted into Petri dish and left dry in the oven at 60 °C for about 24 h. The sample then was further up drying in desiccators filled with silica gel. The composition of $LiNO_3$ and designation of sample for BEs system are tabulated in table 1.

2.2. Characterization of biopolymer electrolytes

2.2.1. Fourier transform infrared spectroscopy (FTIR)

The complexation between alginate and $LiNO_3$ in BEs system were identified by using fourier transform infrared (FTIR) spectroscopy and was recorded using Perkin Elmer Spectrum 100 equipped with an attenuated total reflection (ATR) accessory with a germanium crystal. The sample was tested with the wavenumber in the range of 700 cm^{-1} until 4000 cm^{-1} with spectra resolution of 2 cm^{-1}.

2.2.2. Electrical impedance spectroscopy (EIS)

The ionic conduction of BEs system was analyzed using Electrical Impedance Spectroscopy (EIS). The present sample were cut into a suitable size and sandwiched between two stainless steel (SS) blocking electrodes with surface area is $\pi \text{ cm}^2$ [13]. The conductivity of prepared samples were performed using a HIOKI 3532–50 LCR Hi-Tester with frequency range from 50 Hz to 1 MHz. The ionic conductivity, σ of alginate-$LiNO_3$ BEs system were calculated using equation:-

$$\sigma = \frac{t}{R_b A} \tag{1}$$

where, t (cm) is the thickness, A (cm^2) is the electrode-electrolyte contact area and R_b (Ω) is bulk resistance of BEs system which can be extracted from Cole-Cole plot. The dielectric constant, ε_r (real part of complex permittivity) and loss, ε_i (imaginary part of complex permittivity) can be calculated based on the following equation:

$$\varepsilon_r = \frac{Z_i}{\omega C_o (Z_r{}^2 + Z_i{}^2)} \tag{2}$$

$$\varepsilon_i = \frac{Z_r}{\omega C_o (Z_r{}^2 + Z_i{}^2)} \tag{3}$$

Here $C_o = \varepsilon_o A/t$ is vacuum capacitance, ε_o is permittivity of free space, A is the area of electrode-electrolyte contact, t is the thickness of BEs system. The angular frequency ω is equal to $\omega = 2\pi f$, where f is frequency of applied ac field. Z_r is the real part of impedance and Z_i is the imaginary part of impedance. The real, M_r and imaginary part, M_i of electrical modulus were calculated using the equation below:-

$$M_r = \frac{\varepsilon_r}{(\varepsilon_r{}^2 + \varepsilon_i{}^2)} \qquad (4)$$

$$M_i = \frac{\varepsilon_r}{(\varepsilon_r{}^2 + \varepsilon_i{}^2)} \qquad (5)$$

2.2.3. Transport parameter study

The transport properties of alginate-LiNO$_3$ BEs system were analyzed via FTIR deconvolution. Deconvolution technique was performed using Gaussian-Lorentz function, which adapted from Origin Lab Pro 8.0 software. In this method, the FTIR peaks due to complexation of alginate and LiNO$_3$ were selected based on dominant ionic movement. The area under the peaks was determined, and the free ions percentage (%) were calculated using the equation [14, 15]:

$$Percentage\ of\ free\ ions\,(\%) = \frac{A_f}{A_f + A_c} \times 100\% \qquad (6)$$

where A_f is an area under the peak representing the free ions region, A_c is the total area under the peak representing the contact ions. The transports parameter such as number of mobile ions (η), ionic mobility (μ) and diffusion coefficient (D) were calculated following this equation [16, 17]:-

$$\eta = \frac{MN_A}{V_{Total}} \times free\ ions\,(\%) \qquad (7)$$

where:

$$V_{Total} = \left[\frac{weight}{density}(alginate)\right] + \left[\frac{weight}{density}(LiNO_3)\right] \qquad (8)$$

$$\mu = \frac{\sigma}{\eta e} \qquad (9)$$

$$D = \frac{KT\mu}{e} \qquad (10)$$

where M is number of moles of dopant (LiNO$_3$) used, N_A is the Avogadro's constant (6.02×10^{23} mol^{-1}), V_{total} is total volume of BEs system, k is the Boltzmann constant (1.38×10^{-23} J K^{-1}), T is absolute temperature in Kelvin and e is electric charge (1.602×10^{-19} C).

3. Result and discussion

3.1. IR vibrational study

Figure 1 shows the FTIR spectra for alginate incorporate with various composition of LiNO$_3$. Based on figure 1, it clearly can be seen there is crosslinking reaction between lone pair electrons from alginate and cation from LiNO$_3$ at the groups of C–O–C, COO$^-$, and –OH in the polymer matrix. The highlighted wavenumber which was believed the interaction has occurred between alginate and LiNO$_3$ is presented in figure 2.

In the present work, figure 2(a) denotes the ether group (C–O–C) of alginate-LiNO$_3$ complexes in the region 900 to 1200 cm^{-1}. The absorption peak of BEs system was slight shifting from 1027 cm^{-1} of ALNO-0 to 1030 cm^{-1} of ALNO-3 and remain unchanged until ALNO-5. This indicates the presence of high electronegativity atom (oxygen) from the ether group does not creates any opportunities for interaction occurred between alginate and lithium salt since the ether group form strong bonding in the polymer backbone.

Figure 2(b) depicts another significant peak of alginate-LiNO$_3$ complexes between 1200 to 1800 cm^{-1} which attributed to symmetrical and asymmetrical of carboxylate anion, COO$^-$ [18]. It can be observed that the peak represent to COO$^-$ asymmetric stretching of pure alginate (ALNO-0) shifted to higher wavenumber, from 1596 to 1605 cm^{-1}. It can be explained that with the increment of LiNO$_3$ in BEs system, it will enhance the dissociation of Li$^+$–NO$_3^-$ where positively charged cations from ionic dopant will more attracted to negatively charged of electron pairs from alginate [19]. The changes in wavenumber revealed the complexes between alginate and LiNO$_3$ via weak van der Waals attraction of dipole-dipole forces [20] and this would lead to affect the ionic conduction in BEs system. Besides, the Li$^+$ from LiNO$_3$ function as electrophile positive ion in order to interact with polar group of alginate (Li$^+$…$^-$O) [21]. On the other hand, the absorption peak for COO$^-$ symmetric stretching shifted to lower wavenumber from 1409 to 1400 cm^{-1} which confirms that the migration of Li$^+$ to the coordinating site (oxygen) of COO$^-$ via electrostatic interaction in order to form (Li$^+$…$^-$OOC) [22]. It can be observed that there is appearance of new peak at 1362 cm^{-1} belongs to lithium and nitrate ion stretching which was due to addition of LiNO$_3$ in polymer matrix. This new peak remain unchanged and similar observation was founded in Mobarak (2015) [23] work, where new appearance peak confirmed the presence of
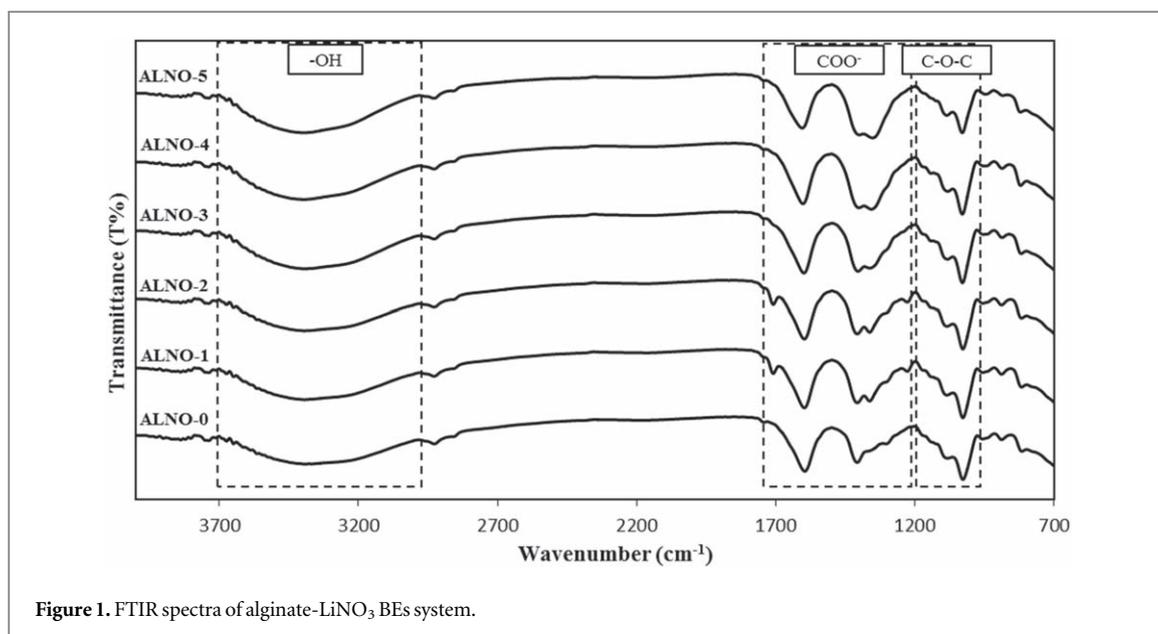
Figure 1. FTIR spectra of alginate-LiNO$_3$ BEs system.
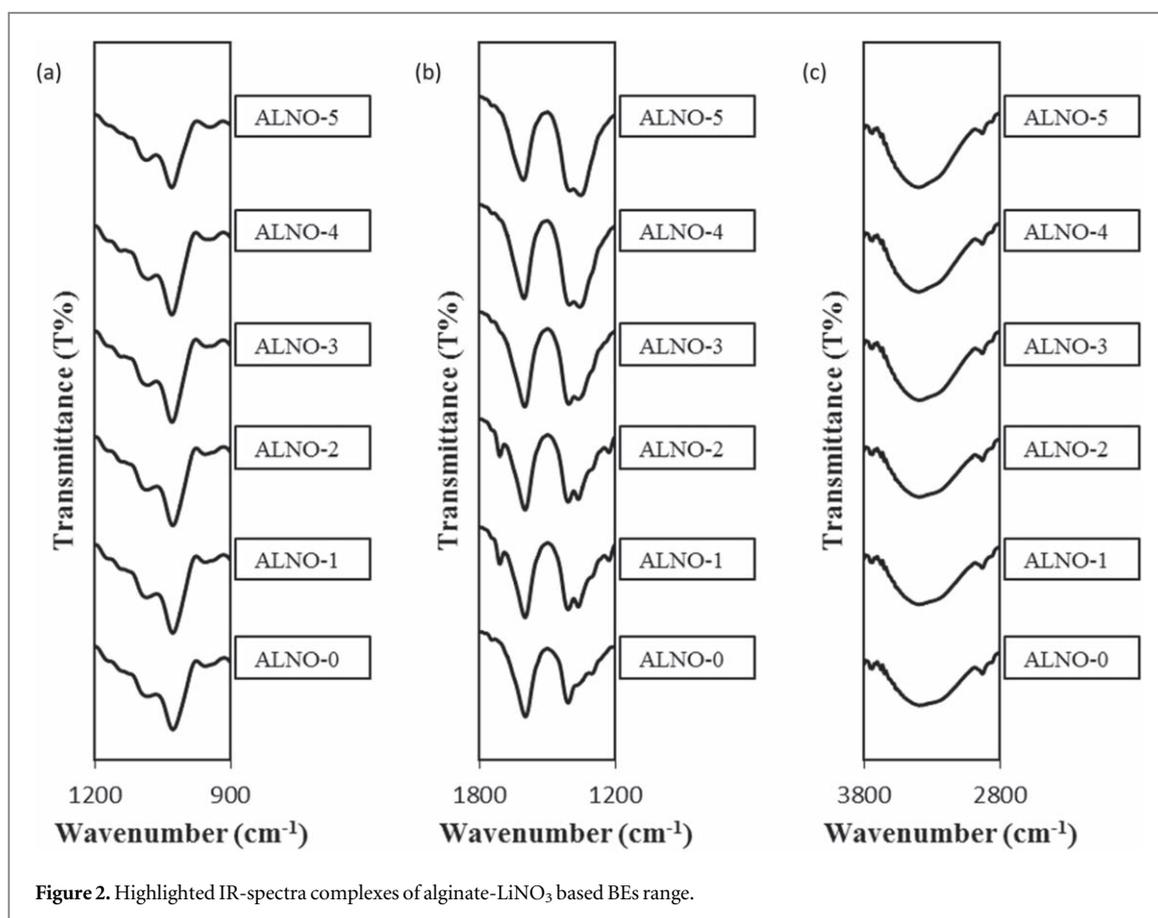
Figure 2. Highlighted IR-spectra complexes of alginate-LiNO$_3$ based BEs range.

ion pairs (Li$^+$ and NO$_3^-$) upon addition of lithium salt and would influences the ionic conductivity of polymer-salt complexes. However, this peak shifted to the lower wavenumber upon addition of salt until sample ALNO-5 and this might due to the aggregation of dopant, which lead to decreasing number of mobile ions; hence, might affect ionic conductivity of BEs system [24].

Meanwhile, figure 2(c) presents FTIR pattern for alginate-LiNO$_3$ complexes in the range from 2800 to 3800 cm^{-1}. The weak peak at 2928 cm^{-1} and strong absorption band at range 3000 to 3600 cm^{-1} were related to CH$_2$ stretching and –OH stretching, respectively [25]. From ATR-FTIR analysis, it can be seen the addition of LiNO$_3$ showed no effect on the intensity or shifting of peak at CH$_2$ stretching. However, the absorption peak of –OH stretching band start to shift from 3368 cm^{-1} for ALNO-0 to higher wavenumber peak at 3390 cm^{-1} for

Table 2. Summary of IR peak in wavenumber for alginate-LiNO$_3$ complexes as BEs system.

Assignment	Wavenumber of BEs system (cm^{-1})						
	LiNO$_3$	ALNO-0	ALNO-1	ALNO-2	ALNO-3	ALNO-4	ALNO-5
Stretching of –OH	—	3368	3393	3393	3396	3396	3396
CH$_2$ stretching	—	2928	2928	2928	2928	2928	2928
Asymmetry of COO$^-$	—	1596	1597	1597	1599	1602	1605
Symmetry of COO$^-$	—	1409	1407	1407	1404	1401	1400
NO$_3^-$ stretching	1403	—	—	—	—	—	—
Li$^+$ stretching	—	—	1362	1362	1362	1356	1352
C–O–C stretching	—	1027	1028	1028	1030	1030	1030

ALNO-3 and remain unchanged until ALNO-5. According to Kadir *et al* (2018) [26], the shifted of polymer complexes to higher wavenumber indicates the dissociation of LiNO$_3$ that lead to the interaction between cation and lone pair of electrons in oxygen atom of hydroxyl group; thus, it expected to increase the number of mobile ions and conductivity in BEs system. The summarization for all changes in functional group of BEs system are tabulated in table 2.

3.2. Ionic conductivity study

According to Rani (2018) [27], impedance spectroscopy is a non-destructive and powerful technique to analyze the conduction properties of polymer electrolytes and their interfaces with electronically conducting electrodes. Figure 3 depicts the Cole-Cole and calculating fitted plots for alginate-LiNO$_3$ BEs at ambient temperature. In the present work, the Cole-Cole plot for a blocking electrode consist of a semicircle and a spike, and only a tilted spike. Based on figure 3, the Cole-Cole plot for ALNO-1, ALNO-2, ALNO-4 and ALNO-5 showed the combination of a tilted semicircle with an inclined (tilted) spike. The semicircle in impedance plot can be represented by parallel combination of bulk resistance, R_b and CPE element with another CPE element in series due to tilted spike; therefore, it confirms the semiconducting behavior [28]. The values of Z_r and Z_i associated to electrical equivalent circuit (EEC) of tilted semicircle and spike can be expressed as:-

$$Z_r = \frac{R + R^2 k_1^{-1} \omega^{p_1} \cos\left(\frac{\pi p_1}{2}\right)}{1 + 2R k_1^{-1} \omega^{p_1} \cos\left(\frac{\pi p_1}{2}\right) + R^2 k_1^{-2} \omega^{2p_2}} + \frac{\cos\left(\frac{\pi p_2}{2}\right)}{k_2^{-1} \omega^{p_2}} \tag{11}$$

$$Z_i = \frac{R + R^2 k_1^{-1} \omega^{p_1} \sin\left(\frac{\pi p_1}{2}\right)}{1 + 2R k_1^{-1} \omega^{p_1} \cos\left(\frac{\pi p_1}{2}\right) + R^2 k_1^{-2} \omega^{2p_2}} + \frac{\sin\left(\frac{\pi p_2}{2}\right)}{k_2^{-1} \omega^{p_2}} \tag{12}$$

where R is bulk resistance, k_1^{-1} is the bulk geometrical capacitance of BEs, k_2^{-1} is the electrical double layer capacitance at the electrode/electrolyte interface during the impedance measurement. The p_1 and p_2 is the ratio of the angle between the diameter of the depressed semicircle from Z_i axis, and p_2 is the skew parameter that controls the degree of the tendency of the title spike from the real axis. From the Cole-Cole plots, the values of parameters k_1 and k_2 were obtained by trial and error method until the fitted points give a good fit to the experimental points. The R_b value is determined from the interception between semicircle arc and the tilted spike with the real axis [29]. The presence of high frequency arc and low frequency spike in the complex impedance plots may be attributed to the bulk conduction process and the accumulation of charges at the electrolyte–electrode (blocking electrode) interface [30]. Here, the depressed semicircle denotes the bulk material while the tilted spike represents the electrical double layer [31]. It can be observed that the incomplete semicircle curve begin to disappear at high frequency and left with only the tilted spike upon higher addition LiNO$_3$. This phenomenon suggests that only the resistive component of the electrolyte prevails [32]. On the other hand, sample ALNO-3 shows the fully inclined spike in the impedance study. So, the values of Z_r and Z_i associated to EEC of only tilted spike can be expressed as:-

$$Z_r = R_b + \frac{k_2 \cos\left(\frac{\pi p_2}{2}\right)}{\omega^p} \tag{13}$$

Figure 3. Cole-Cole plot with equivalent circuit for sample (a) ALNO-1, (b) ALNO-2, (c) ALNO-3, (d) ALNO-4, and (e) ALNO-5 of BEs system at ambient temperature.
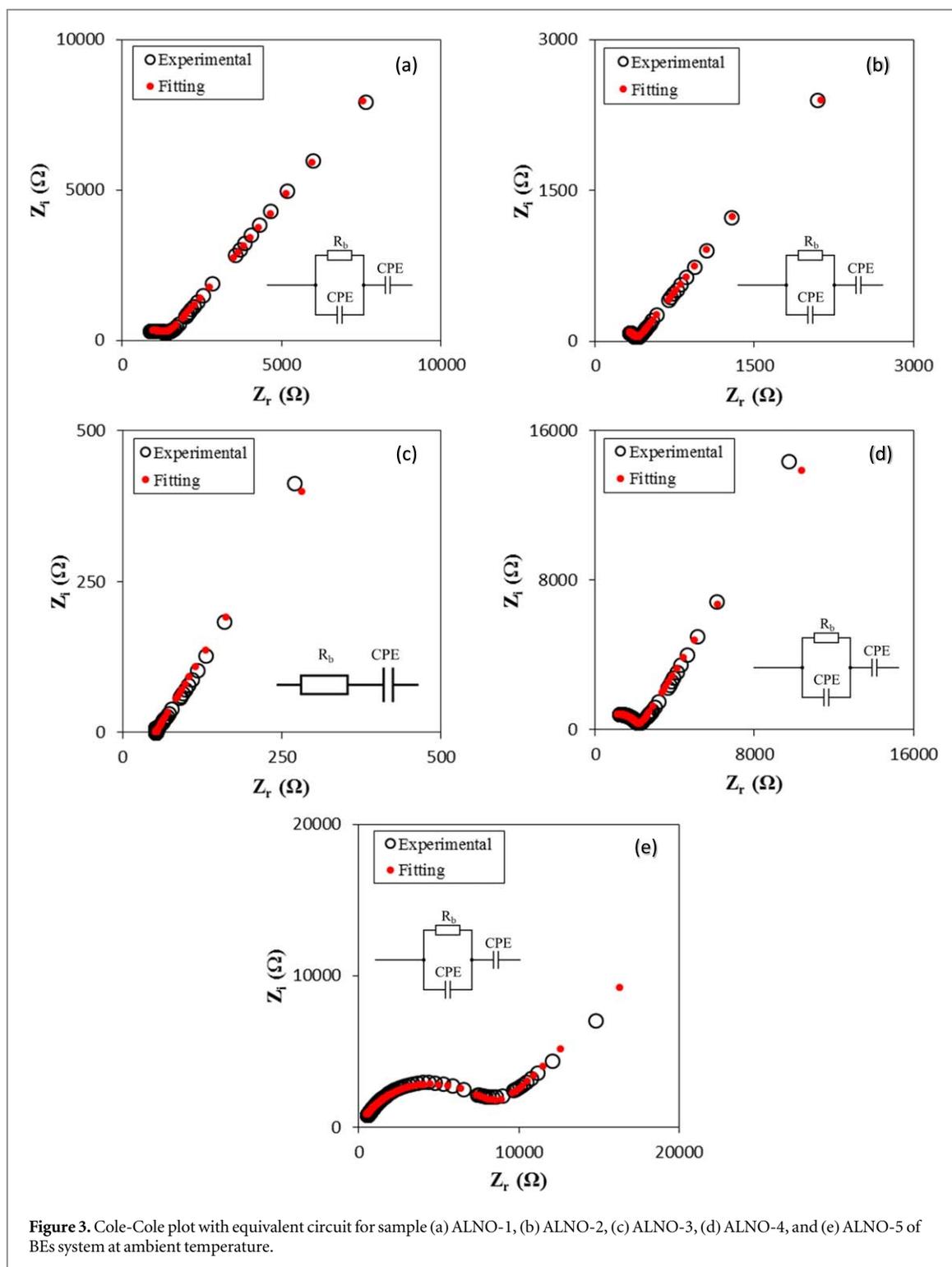
$$Z_i = \frac{k_2 \sin\left(\dfrac{\pi p_2}{2}\right)}{\omega^P} \tag{14}$$

Since the spike in this study did not begin at the origin, the equivalent circuit is consist of a resistor and constant phase element (CPE) in series connection. CPE for the spike is due to the double-layer capacity of an inhomogeneous electrode surface [33]. A resistor in series with a CPE can represent the plot that takes the shape of a spike. Based on figure 3(c), ALNO-3 showed fully inclined spike with disappearance of incomplete semicircle and shifted to lower value attributable to dissociation of $LiNO_3$, which enables the free ions to participate in conduction process [34]. The calculated values of theoretical fitting parameter are presented in

Figure 4. Ionic conductivity and activation energy for alginate-LiNO$_3$ BEs system at ambient temperature.

Figure 5. Ionic conductivity of alginate-LiNO$_3$ BEs system at different temperature.
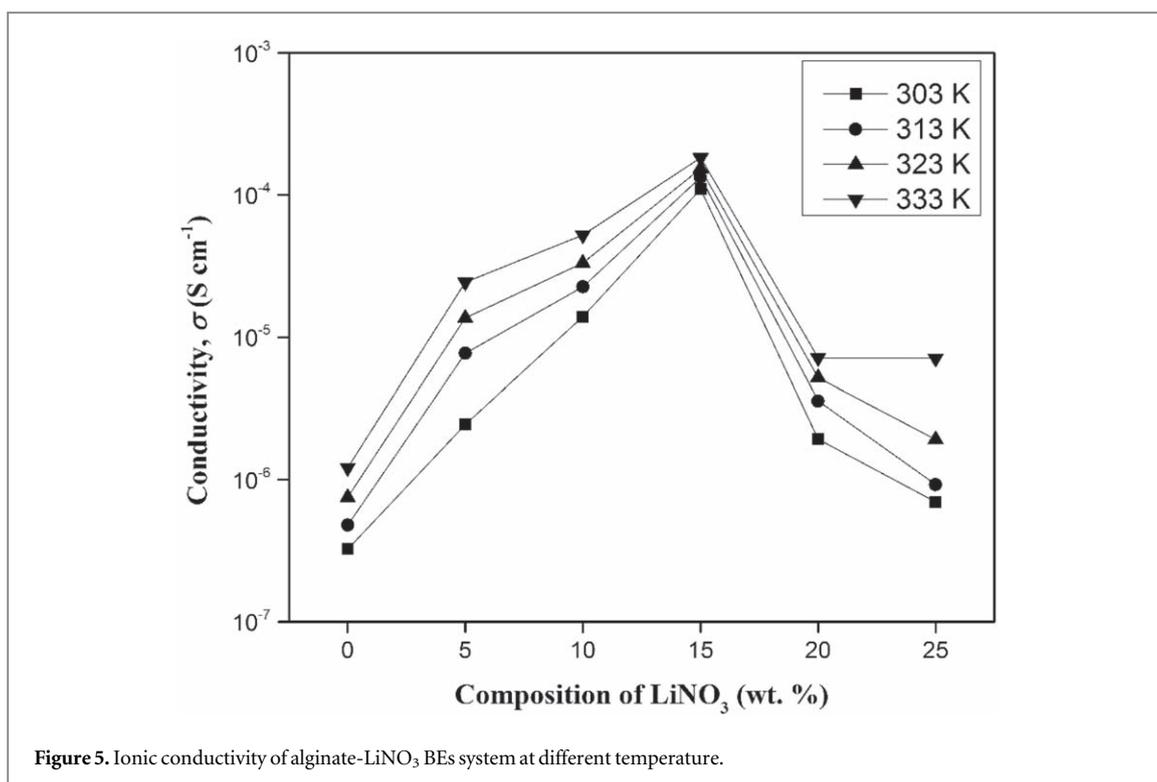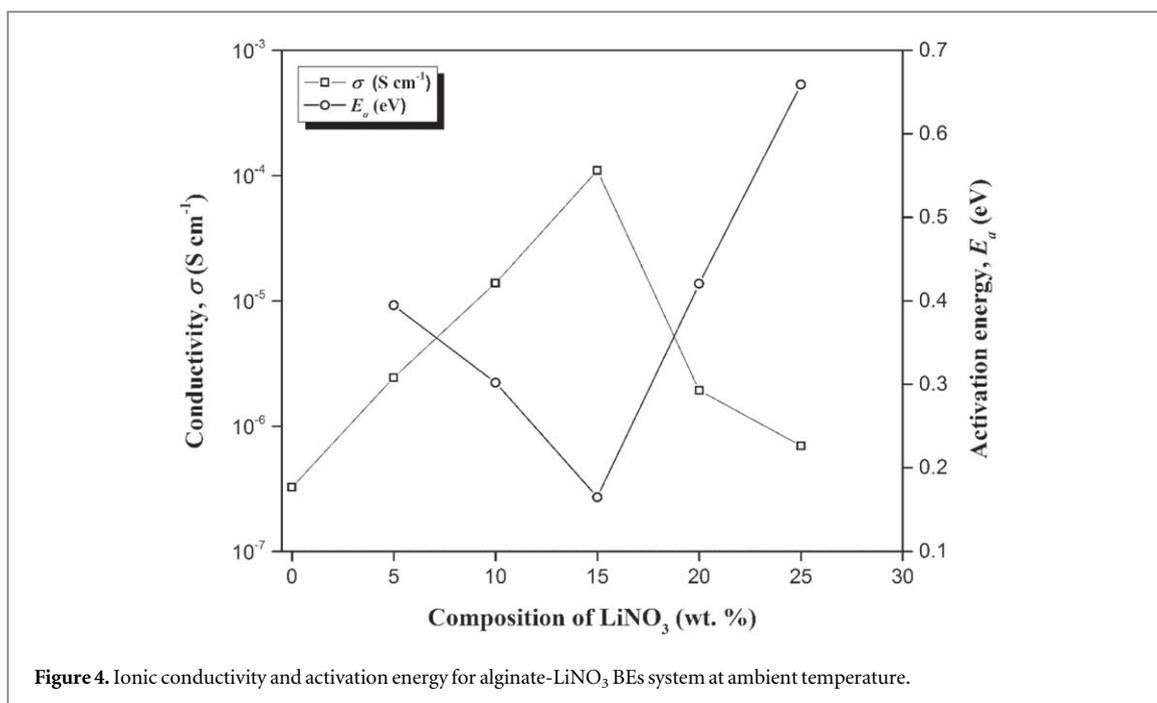
Table 3. The t, R_b and fitting parameters (p_1, k_1, p_2, and k_2) of BEs system.

Sample	Thickness, t (cm)	R_b (Ω)	p_1	k_1 (F^{-1})	p_2	k_2 (F^{-1})
ALNO-1	0.0085	1369	0.58	21,850,000	0.58	533,500
ALNO-2	0.0105	390	0.72	94,300,000	0.60	93,950
ALNO-3	0.0170	51	—	—	0.67	21,593
ALNO-4	0.0178	2164	0.81	720,000,000	0.66	719,500
ALNO-5	0.0131	8550	0.73	94,990,000	0.54	271,500

Figure 6. Arrhenius plot for alginate-LiNO$_3$ BEs system.

Figure 7. (a) Dielectric constant and (b) dielectric loss of alginate-LiNO$_3$ BEs system at ambient temperature.
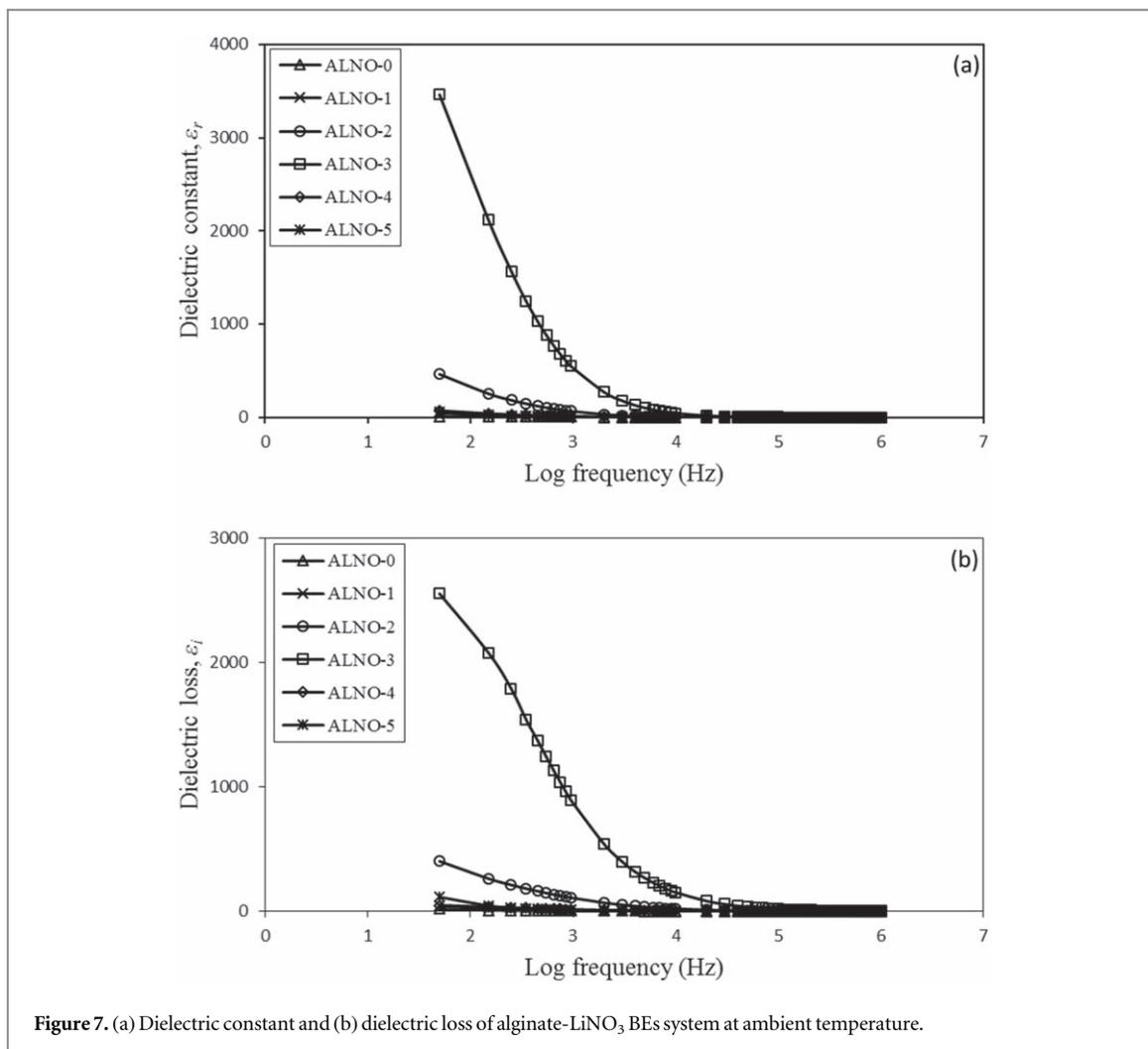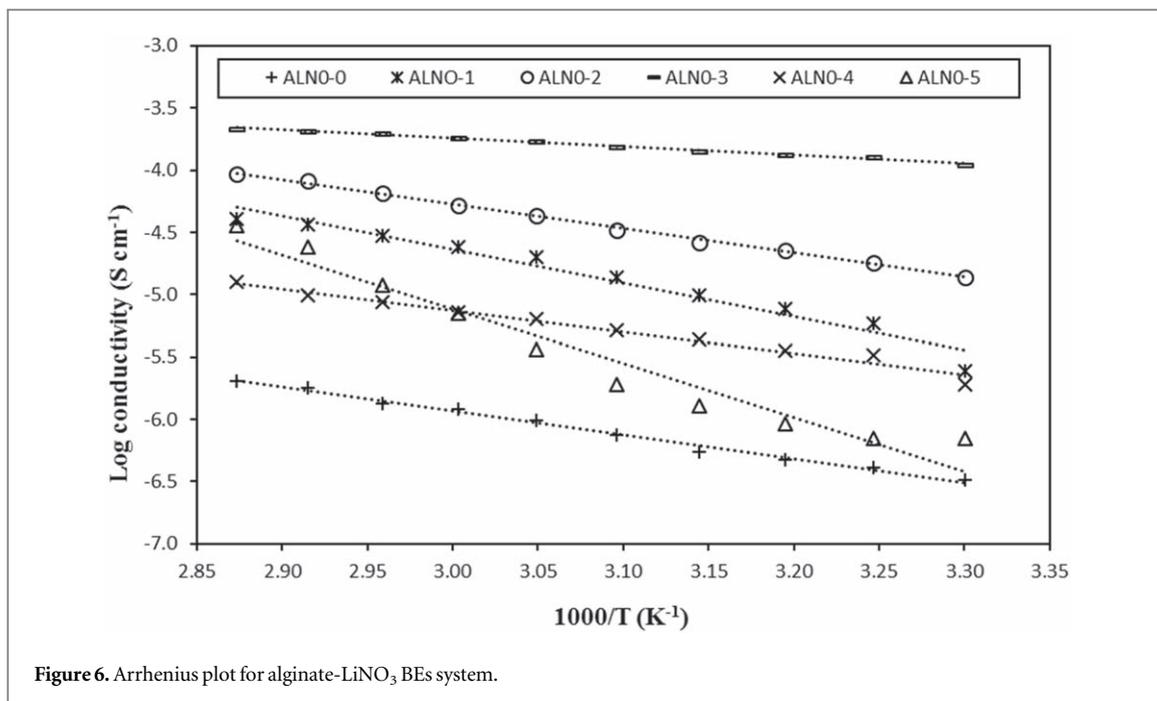
table 3. It clearly can be seen that the R_b value for ALNO-3 exhibits the minimum value of 51 Ω indicates that the sample becomes more capacitive than resistive [35]. Therefore, the fully inclined spike of sample ALNO-3 were expected to have higher conductivity value in BEs system.

Figure 8. (a) Dielectric constant and (b) dielectric loss for ALNO-3 at different temperature.
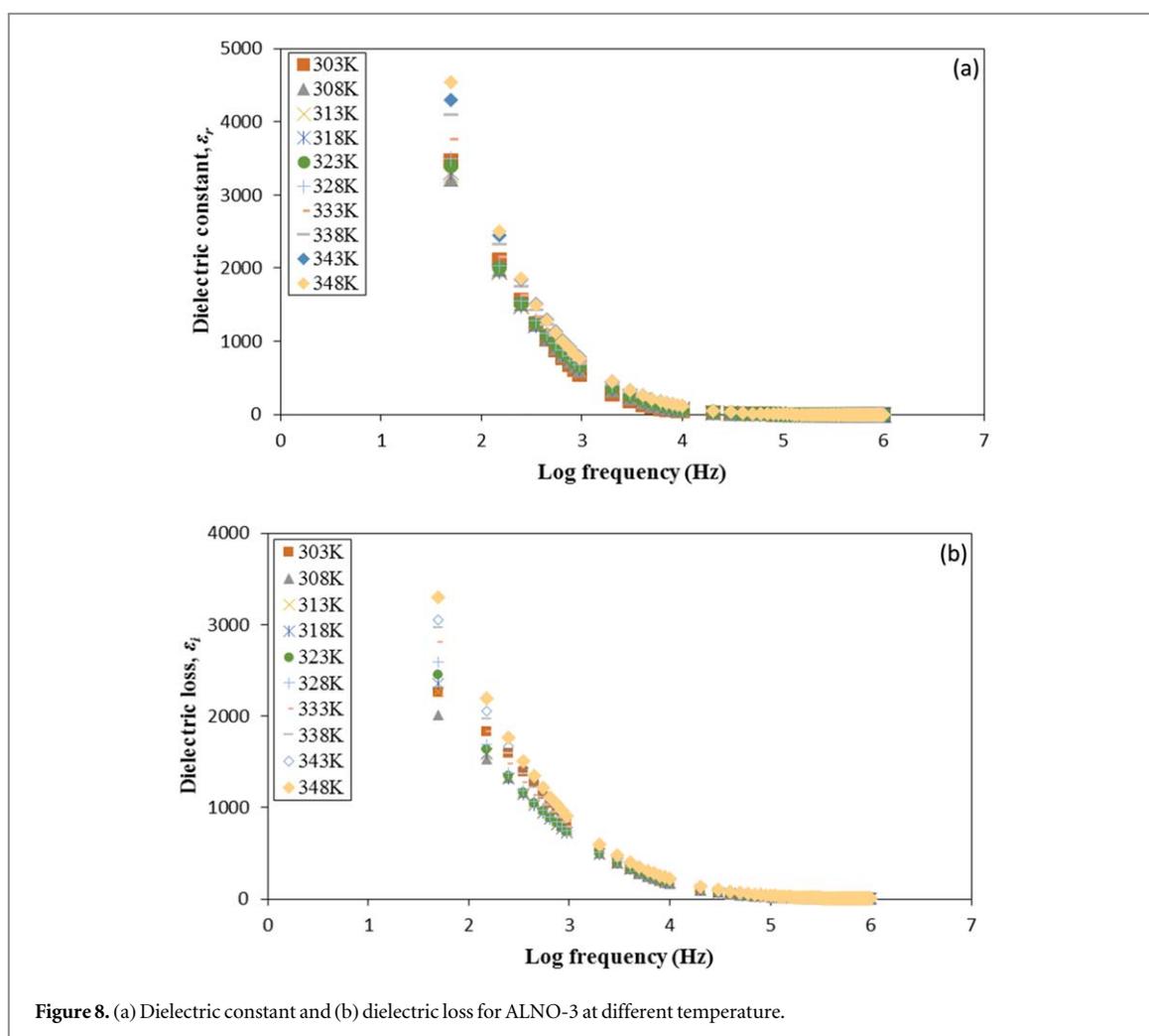
Table 4. Dielectric part for various BEs system.

Polymer electrolytes	ε_r (303 K) at 10 000 Hz	ε_i (303 K) at 10 000 Hz	References
Chitosan/PVA-LiClO$_4$	~3.5	~6.75	[48]
Starch/chitosan-NH$_4$Cl	~50	~90	[49]
Cellulose acetate-LiNO$_3$	~500	~900	[11]
Pectin-LiCl	~1800	~1200	[50]
Alginate-LiNO$_3$	~436	~1550	Present work

The ionic conductivity value for entire sample of alginate-LiNO$_3$ BEs system at ambient temperature is presented in figure 4. The remarkable effect with incorporation of LiNO$_3$ enhanced the ionic conductivity by three order of magnitude until achieved optimum value at 1.10×10^{-4} S cm^{-1} for sample containing 15 wt% of LiNO$_3$ (ALNO-3). Alves *et al* (2018) [36] proclaim that ionic conductivity mainly affected by three factor which are (i) types of cation and anion, (ii) salt composition, and (iii) temperature. Generally, increment of LiNO$_3$ in BEs system cause the ionic conductivity to improved which was due to the concentration of mobile charge carriers from Li$^+$. This also can be proven as discussed earlier in FTIR analysis, increment addition of LiNO$_3$ provide more cation to attracted with potential coordinating of alginate thus, the ionic conductivity will affected. It shows that addition above 15 wt. % of LiNO$_3$ lead to decreasing in ionic conductivity of BEs and this might due to the aggregation of ion cluster appeared at high level and increase the formation of overcrowded ions in system.

The ionic conductivity for entire sample at various are presented in figure 5. It can been observed that the ionic conductivity increased with increasing temperature for entire sample. This was due to the formation of free volume provided by alginate from their chain and created unoccupied spaces for migration of ions [37]. The enhancement of ionic conductivity is also attributed to overall mobility of ion and polymer which determined by the free volume; hence, it will leads to the increased in ionic and segmental mobility that will assist ion transport and practically compensate the retarding effect of ion clouds [38]. The segmental motion of the polymer chain
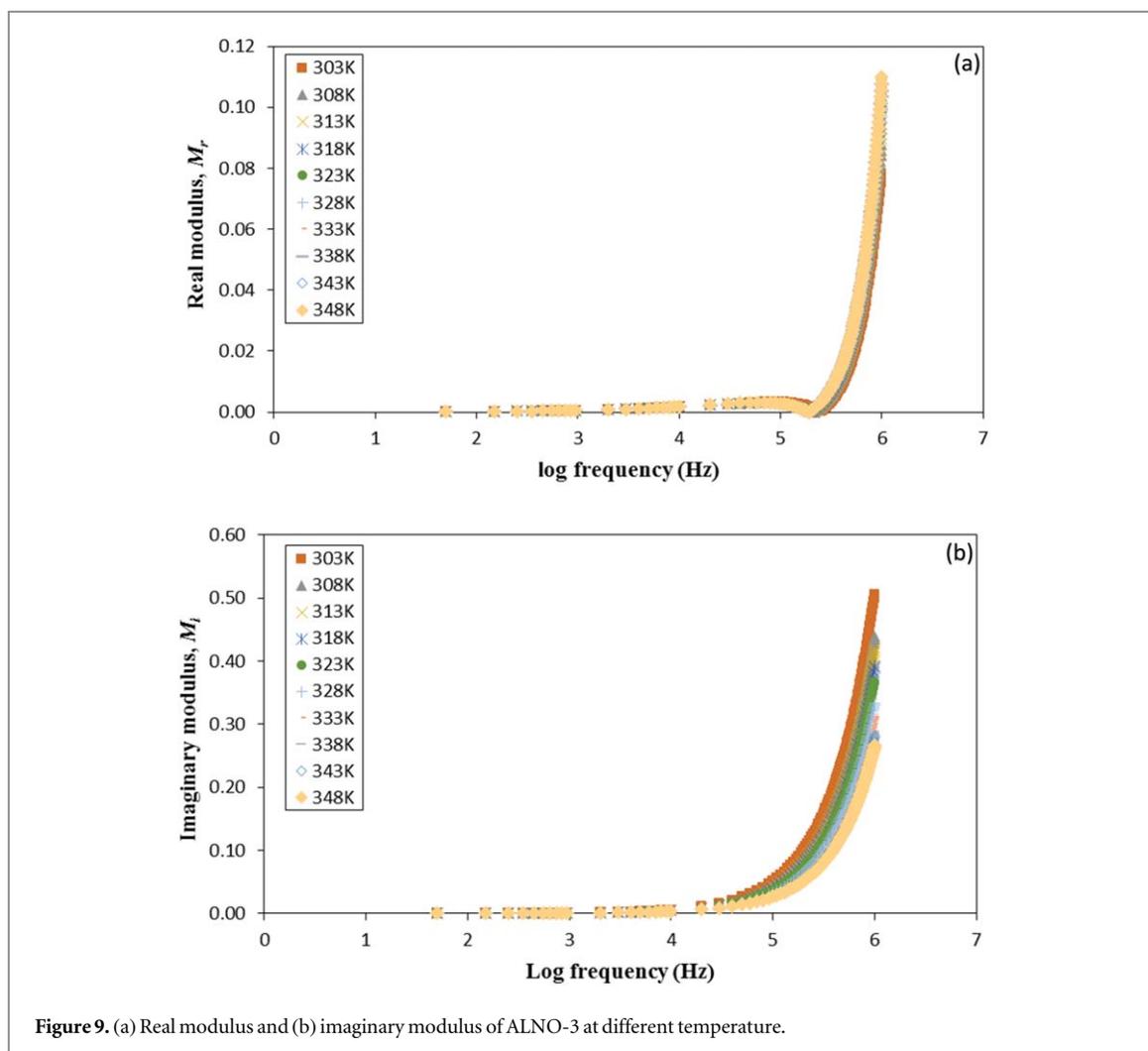
Figure 9. (a) Real modulus and (b) imaginary modulus of ALNO-3 at different temperature.

and dissociation of the dopant increased due to vibrational energy occurred in the space around its own volume of which believed to push against the hydrostatic pressure imposed by its neighboring atoms [39]. Therefore, the particles move unreservedly in the free volume around the polymer chain and lead to the enhancement of the ionic conductivity value [40]. Figure 6 depicts the log conductivity versus 1000/T for various BEs sample at the temperature range from 303 K to 348 K. It can be seen that all regression values are close to unity suggesting that the points lie on fitting lines, so the variations of conductivity with temperature is obey with the Arrhenius rule [41]:-

$$\sigma = \sigma_o \exp\left(-\frac{E_a}{k_b T}\right) \qquad (15)$$

where E_a is the activation energy, σ is the ionic conductivity of BEs system, σ_0 is the pre-exponential factor, k_b is the Boltzmann constant, and T is the temperature in Kelvin. Figure 4 shows the activation energy for various composition of LiNO$_3$ at ambient temperature. The E_a was found to be decreases as the ionic conductivity of BEs increased due to higher flexibility of the alginate backbone based on enhancement of segmental mobility of its chains [42]. Therefore, it requires low activation energy to facilitates the motion of ions in the biopolymer network [43].

3.3. Electrical study
Dielectric properties provide an important insight regarding on conduction complexes behavior in BEs system. The dielectric properties may vary in different types of polymer electrolyte system attributed to several factors including frequency of applied electrical field, temperature, structural characteristics or other external factors [44]. The variation of ε_r and ε_i as function of frequency at ambient temperature are shown in figures 7(a) and (b) respectively.

It is clear can be seen from both figures where the value of ε_r and ε_i are higher at low frequency region due to presence of polarization effect which confirms non-Debye dependence [45]. In this work, both values of ε_r and ε_i

Figure 10. The IR deconvolution spectrum for samples (a) ALNO-1, (b) ALNO-2, (c) ALNO-3, (d) ALNO-4, and (e) ALNO-5 of BEs system.
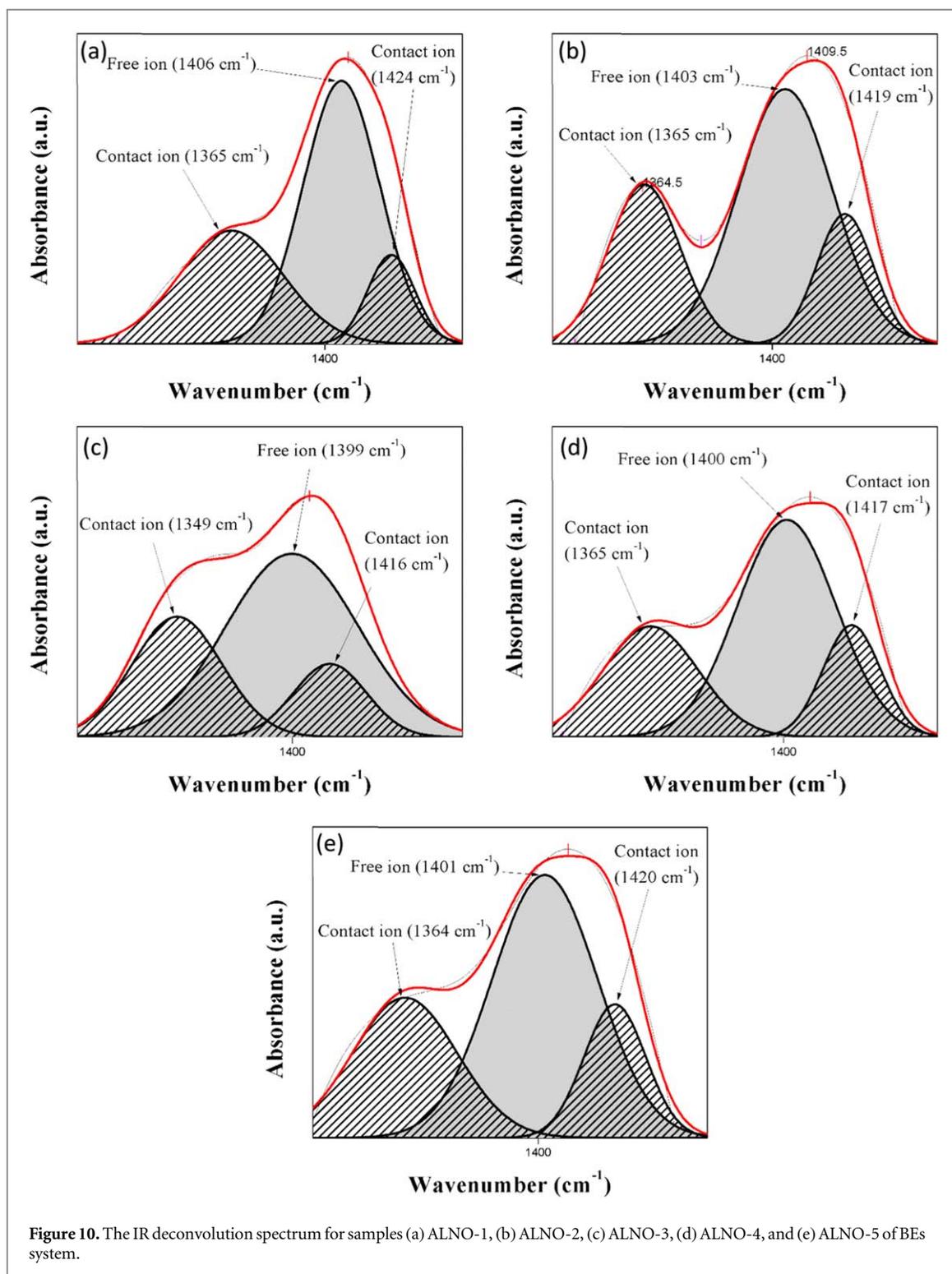
were found to be higher for sample ALNO-3 and this attributable to increment in charge carrier concentration which lead the ionic conductivity to achieved optimum value [11]. At high frequencies, it can be observed both dielectric profiles are decreased and reached plateau conditon for entire samples. This mechanism might be due to the higher periodic reversal of the applied field where there is no charge build up at the interface between the sample and the electrode (space-charge) and also no excess ion diffusion in the path of field [46, 47].

Figure 8 depicts the temperature dependence of ε_r and ε_i for most conducting sample in BEs system (ALNO-3). It can be observed that both ε_r and ε_i of BEs system increased with increasing of temperature and this is due to the polarization of the mobile ions. As the temperature increased, degree of $LiNO_3$ dissociation and re-dissociation of ion aggregates increases due to higher content of free ions or charge carrier density; thus, it will lead to enhancement of ionic conductivity with temperature [46]. Table 4 showed the dielectric part from the literature as comparison for the present highest conducting BEs system. Its revealed that the present BEs is

Figure 11. Free ions and contact ions of alginate-LiNO$_3$ BEs system.

Figure 12. Transport parameters and conductivity of alginate-LiNO$_3$ BEs system.
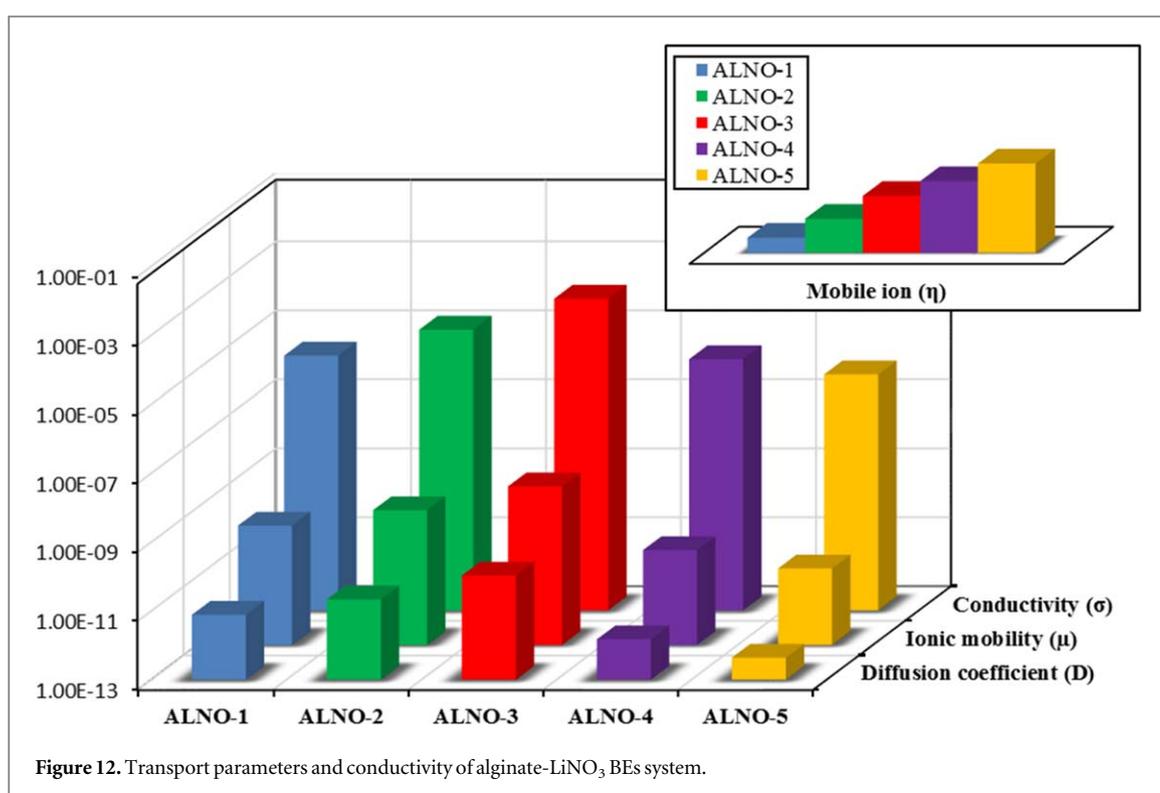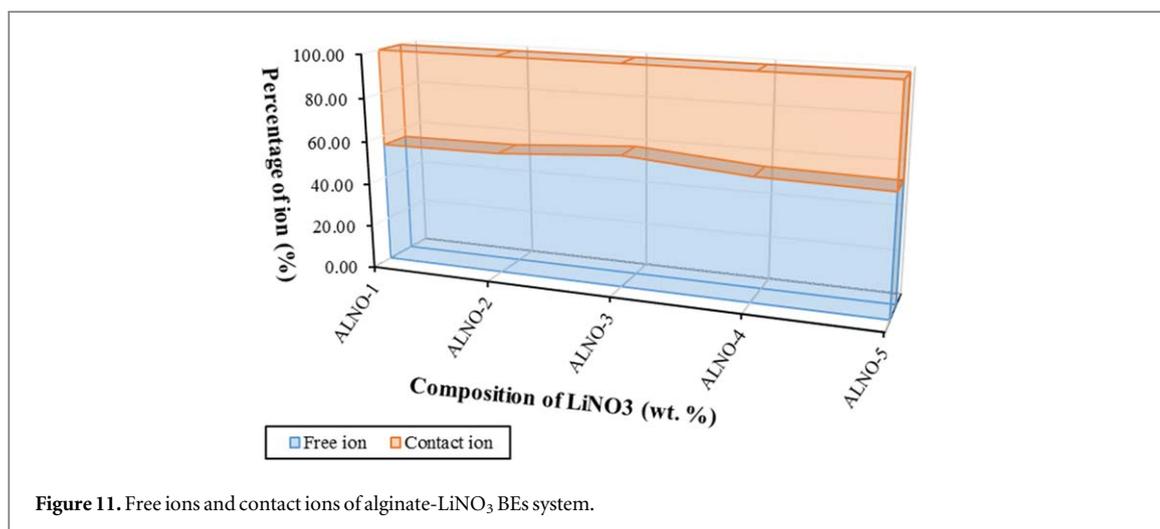
comparable with other types of polymer electrolytes system which implies their capability to stored a charge when apply in energy devices. A further investigation of the dielectric behavior can be more successfully achieved using a modulus formalism analysis.

The real and imaginary part of modulus spectrum for ALNO-3 exhibited as shown in figure 9. Based on figure 9, both M_r and M_i values are increased at higher frequency region without any relaxation peak was observed. Increasing value for both modulus part is due to the distribution of relaxation processes over a range of frequencies [51]. In addition, a long tail at low frequencies depicts that there might be a large capacitance associated with the electrodes polarization effects which further confirms non-Debye behavior in the samples [52, 53]. According to Bakar *et al* (2015) [54], modulus part increase as frequency increase due to bulk polarization which can be differentiate into two elements; (i) transferred by electron and (ii) avalanche transit-time. In the present work, it is believed the bulk effects appeared in the complexes due to transferred by electron between host polymer and ionic dopant.

3.4. Transport properties study

Figure 10 depicts the FTIR deconvolution for various composition LiNO$_3$. According to Ren *et al* (2016) [55], strong absorption peaks at ~1400 cm^{-1} denotes the anion vibration mode of NO$_3^-$ which proved the IR active in

FTIR study. Arya *et al* (2019) [56] also reported that NO_3^- mode confirms the D_{3h} point group and the fundamental modes proved that peak at 1380 cm^{-1} were correspond to asymmetric stretching of NO_3^- for LiNO$_3$. Therefore, the band of NO_3^- showed great importance for the investigation of ions dissociation in BEs system. In this work, the region between 1200 cm^{-1} to 1500 cm^{-1} were selected due to obvious ions interaction occurred in alginate-LiNO$_3$. Thus, the peak located at $\sim$1400 cm^{-1} of LiNO$_3$ is believed due to the free anion (resulting from dissociation of ions) while peak located at $\sim$1350 cm^{-1} and $\sim$1420 cm^{-1} were attributed to contact ions (due to association of ions) which can be ion pairs or ion aggregates [57]. Figure 11 presents the percentage of free ions and the contact ions of alginate-LiNO$_3$ BEs system.

It can be observed that the percentage of free ions increases and the percentage of contact ions decreases when LiNO$_3$ was added. The highest percentage of free ions was obtained for the optimum ionic conductivity of BEs system. This implies that more ions are dissociated and would provide with balanced interactions between alginate and LiNO$_3$; thus, assisting more ion conduction in BEs system [58]. The calculated value of the ionic mobility (μ) and the diffusion coefficient number (D) and the number of mobile ions (η) of the BEs were depicted in figure 12.

Based on figure 12, the value μ and D were found to be similar with the trend of ionic conductivity where it rise sharply at ALNO-3 with maximum value of 4.07×10^{-9} cm^2 V^{-1} s^{-1} and 1.06×10^{-10} cm^2 s^{-1}, respectively. In the present work, addition of LiNO$_3$ in alginate definite the conjecture in FTIR study where the diffusion of Li$^+$ from LiNO$_3$ and migrate to lone pair of COO$^-$ of alginate contain with huge amount of ions and also faster rate. The μ and D will lead to the enhancement of ionic conductivity where it need lesser activation energy to hopping in the backbone of alginate [59]. Referring to figure 12, it can be inferred that the number of η increased linearly upon addition higher composition of LiNO$_3$ and this was attributed to the dissociation of dopant which lead to the overcrowding of mobile ions that obstruct the pathway for migration process; thus, the value of μ and D decreased [60].

4. Conclusion

In the present work, a favorable measured data of biopolymer electrolytes (BEs) based on alginate incorporate with lithium nitrate (LiNO$_3$) have been successfully prepared via solution casting technique. From FTIR analysis, there are presence of new peak appeared near at symmetric COO$^-$ ($\sim$1360 cm^{-1}) of alginate indicates there are interaction between polymer matrix and ionic dopant. The ionic conductivity of alginate-LiNO$_3$ at ambient temperature exhibits optimum value at 1.10×10^{-4} S cm^{-1} for 15 wt. % of LiNO$_3$ (ALNO-3). The temperature dependence of conductivity was found to obey the Arrhenius behavior. The dielectric behavior of BEs system were characterized by using complex permittivity and electrical modulus and shown non-Debye behavior. Based on IR-deconvolution technique, it shown the ionic conductivity of BEs is governed by mobile ions (μ) and the diffusion coefficient number (D). Based on present results, it can be concluded that the biopolymer namely alginate, showing good potential to act as host polymer, which can be used as an electrolyte for application in electrochemical devices.

Acknowledgments

ORCID iDs

A S Samsudin ⬤ https://orcid.org/0000-0001-7472-2530

References

[1] Muthukrishnan M, Shanthi C, Selvasekarapandian S, Manjuladevi R, Perumal P and Chrishtopher Selvin P 2018 *Ionics* **25** 203–214
[2] Tudu K, Pal S and Mandre N R 2018 *International Journal of Minerals, Metallurgy, and Materials* **25** 498–504
[3] Schintu M, Meloni P and Contu A 2000 *Ecotoxicol. Environ. Saf.* **46** 29–33
[4] Singh R, Singh P K, Tomar S K and Bhattacharya B 2016 *High Perform. Polym.* **28** 47–54
[5] Shankar S, Wang L-F and Rhim J-W 2016 *Carbohydr. Polym.* **146** 208–16
[6] Lacoste C, El Hage R, Bergeret A, Corn S and Lacroix P 2018 *Carbohydr. Polym.* **184** 1–8
[7] Wang L-F, Shankar S and Rhim J-W 2017 *Food Hydrocolloids* **63** 201–8
[8] Duan H, Yin Y-X, Zeng X-X, Li J-Y, Shi J-L, Shi Y, Wen R, Guo Y-G and Wan L-J 2018 *Energy Storage Mater.* **10** 85–91

[9]   Manjuladevi R, Selvin P C, Selvasekarapandian S, Shilpa R and Moniha V 2018 *AIP Conference Proceedings* **1942** 140075
[10] Yahya M Z A and Arof A K 2004 *Carbohydr. Polym.* **55** 95–100
[11] Monisha S, Mathavan T, Selvasekarapandian S and Benial A M F 2017 *Ionics* **23** 2697–706
[12] Ramesh S, Shanti R and Morris E 2012 *Carbohydr. Polym.* **87** 2624–9
[13] Samsudin A S and Isa M I N 2012 *Int. J. Polymer. Mater.* **61** 30–40
[14] Zainuddin N K and Samsudin A S 2018 *Mater. Today Comm.* **14** 199–209
[15] Winie T, Shahril N S M, Chan C H and Arof A K 2014 *High Perform. Polym.* **26** 666–71
[16] Salleh N S, Aziz S B, Aspanut Z and Kadir M F Z 2016 *Ionics* **22** 2157–67
[17] Rasali N M J and Samsudin A S 2017 *Ionics* **24** 1–12
[18] Sellimi S, Younes I, Ayed H B, Maalej H, Montero V, Rinaudo M, Dahia M, Mechichi T, Hajji M and Nasri M 2015 *Int. J. Biol. Macromol.* **72** 1358–67
[19] Shukur M F, Hamsan M H and Kadir M F Z 2018 *Journal of Physics: Conference Series* **1123** 012001
[20] Mazuki N F, Fuzlin A F, Saadiah M A and Samsudin A S 2018 *Ionics* **25** 2657–67
[21] Monisha S, Mathavan T, Selvasekarapandian S, Benial A M F, Aristatil G, Mani N and Premalatha M 2017 *Carbohydr. Polym.* **157** 38–47
[22] Bar N, Basak P and Tsur Y 2017 *PCCP* **19** 14615–24
[23] Mobarak N N, Jumaah F N, Ghani M A, Abdullah M P and Ahmad A 2015 *Electrochim. Acta* **175** 224–31
[24] Sohaimy M I H and Isa M I N 2015 *Fibers Polym.* **16** 1031–4
[25] Xu J, Zhang C, Ge T, Dai Y and Wang R 2018 *Appl. Therm. Eng.* **128** 214–24
[26] Kadir M F Z, Salleh N S, Hamsan M H, Aspanut Z, Majid N A and Shukur M F 2018 *Ionics* **24** 1651–62
[27] Rani M S A, Ahmad A and Mohamed N S 2018 *Polym. Bull.* **75** 5061–74
[28] Zainuddin N K, Saadiah M A, Abdul Majeed A P P and Samsudin A S 2018 *Int. J. Polym. Anal. Charact.* **23** 321–30
[29] Arof A K, Amirudin S, Yusof S Z and Noor I M 2014 *PCCP* **16** 1856–67
[30] Chowdhury F I, Khandaker M U, Amin Y M, Kufian M Z and Woo H J 2017 *Ionics* **23** 275–84
[31] Baharun N N S, Mingsukang M A, Buraidah M H, Woo H J and Arof A K 2018 *20th International Conference on Transparent Optical Networks (ICTON)* 1–4
[32] Shukur M F, Ithnin R and Kadir M F Z 2014 *Electrochim. Acta* **136** 204–16
[33] Shamsuddin L, Noor I M, Albinsson I, Mellander B and Arof A K 2017 *Mol. Cryst. Liq. Cryst.* **655** 181–94
[34] Neto M J, Leones R, Sentanin F, Esperanca J M S S, Medeiros M J, Pawlicka A and Silva M M 2014 *J. Electroanal. Chem.* **714** 63–9
[35] Shuhaimi N E A, Teo L P, Woo H J, Majid S R and Arof A K 2012 *Polym. Bull.* **69** 807–26
[36] Alves R, Sentanin F, Sabadini R C, Fernandes M, de Zea Bermudez V, Pawlicka A and Silva M M 2018 *Electrochim. Acta* **267** 51–62
[37] Francis K M G, Subramanian S, Shunmugavel K, Naranappa V, Pandian S S M and Nadar S C 2016 *Polym. Plast. Technol. Eng.* **55** 25–35
[38] Pradeepa P, Sowmya G, Kalaiselvimary J and Prabhu M R 2016 *Mater. Sci. Eng.: B* **205** 6–17
[39] Sundaramahalingam K, Vanitha D, Nallamuthu N, Manikandan A and Muthuvinayagam M 2018 *Physica B: Condens. Matter.* **553** 120–6
[40] Sampathkumar L, Selvin P C, Selvasekarapandian S, Perumal P, Chitra R and Muthukrishnan M 2019 *Ionics* **25** 1067–82
[41] Polu A R, Kumar R and Rhee H 2014 *High Perform. Polym.* **26** 628–31
[42] Che Balian S R, Ahmad A and Mohamed N S 2016 *Polym.* **8** 163
[43] Hemalatha R, Alagar M, Selvasekarapandian S, Sundaresan B, Moniha V, Boopathi G and Selvin P C 2019 *Ionics* **25** 141–54
[44] Saadiah M A and Samsudin A S 2018 *IOP Conference Series: Materials Science and Engineering* **342** 012045
[45] Kumaran V S, Ng H M, Ramesh S, Ramesh K, Vengadaesvaran B and Numan A 2018 *Ionics* **24** 1947–53
[46] Rani M S A, Mohamed N S and Isa M I N 2015 *Int. J. Polym. Anal. Charact.* **20** 491–503
[47] Rasali N M J, Muzakir S K and Samsudin A S 2017 *Makara J. Tech.* **21** 65–9
[48] Rathod S G, Bhajantri R F, Ravindrachary V, Pujari P K and Sheela T 2014 *Journal of Advanced Dielectrics* **4** 1450033
[49] Shukur M F, Ithnin R and Kadir M F Z 2014 *Ionics* **20** 977–99
[50] Perumal P, Selvin P C and Selvasekarapandian S 2018 *Ionics* **24** 3259–70
[51] Rani M S A, Dzulkurnain N A, Ahmad A and Mohamed N S 2015 *Int. J. Polym. Anal. Charact.* **20** 250–60
[52] Isa M I N and Samsudin A S 2017 *Int. J. Polym. Anal. Charact.* **22** 447–54
[53] Fuzlin A F, Rasali N M J and Samsudin A S 2018 *IOP Conference Series: Materials Science and Engineering* **342** 012080
[54] Bakar N Y, Hafiza M N, Bashirah A N A and Isa M I N 2015 *American Journal of Applied Sciences* **12** 40
[55] Ren Z, Xu X, Wang X, Gao B, Yue Q, Song W, Zhang L and Wang H 2016 *J. Colloid Interface Sci.* **468** 313–23
[56] Arya A and Sharma A L 2019 *J. Mater. Sci.* **54** 7131–55
[57] Noor N A M and Isa M I N 2019 *Int. J. Hydrogen Energy* **44** 8298–306
[58] Chai M N and Isa M I N 2016 *Scientific reports* **6** 27328
[59] Rasali N M J, Nagao Y and Samsudin A S 2018 *Ionics* **25** 641–5
[60] Sohaimy M I H and Isa M I N 2017 *Polym. Bull.* **74** 1371–86